International Journal of Heat and Mass Transfer 52 (2009) 5978–5989

Contents lists available at ScienceDirect

International Journal of Heat and Mass Transfer

journal homepage: www.elsevier.com/locate/ijhmt

Heat transfer and fluid flow in shrouded pin fin arrays with and without tip clearance

Kevin A. Moores [a,*], Jungho Kim [a], Yogendra K. Joshi [b]

[a] Department of Mechanical Engineering, University of Maryland, College Park, MD 20742, United States
[b] G.W. Woodruff School of Mechanical Engineering, Georgia Institute of Technology, Atlanta, GA 30332, United States

ARTICLE INFO

Article history:
Received 30 January 2009
Received in revised form 10 August 2009
Available online 7 September 2009

Keywords:
Pin fin
Liquid cooling
Tip clearance
Liquid crystal
Heat transfer

ABSTRACT

Shrouded pin fin arrays with tip clearances (Cg) up to 25% of pin height were experimentally evaluated. Pressure loss was measured ($2 \times 10^2 < Re_D < 2 \times 10^4$) and liquid crystal thermography was employed to obtain temperature distributions from which the impact of Cg on the mean heat transfer rate was determined for $2 \times 10^2 < Re_D < 1 \times 10^4$. Cg was found to influence pressure drop performance to the greatest extent at low Re_D, ($<5 \times 10^3$), with the effect being significantly diminished by $Re_D = 1.5 \times 10^4$. On a per unit pumping power basis, higher heat transfer rates were observed for dimensionless clearances (Cg/D) less than 0.2 as compared to the non-clearance case.

1. Introduction

A typical shrouded pin array (Fig. 1a), consists of a collection of uniformly spaced cylindrical fins, which extends from a base area and is closely constrained by opposing walls on all other sides. Over the past 25 years, a substantial amount of research has been conducted on heat transfer and fluid flow associated with shrouded pin fin arrays. In particular, arrays of short pins with height-to-diameter (H/D) ratios on the order of 1 have been studied extensively as they relate to the cooling of the trailing edge of a turbine blade which historically has been the primary focus and motivation for studying these geometries.

In such applications, the pins are cast into the interior of the blade, span the full height of the blades (Fig. 1b), and are integral to its structural integrity while also enhancing heat transfer. The scenario in which tip clearance is present (Fig. 1c), is typically not a feature of consideration in turbine blades, and has received relatively little attention in the literature. Microelectronics cooling is another area in which shrouded pin fin arrays are employed to augment heat transfer. In order to handle the high heat generation rates, many of today's most advanced power semiconductor modules depend on forced liquid cooling solutions employing arrays that are geometrically similar to those in turbine blades. In this scenario, however, the array typically protrudes from the base of a heat sink and is not required to perform a structural role, allowing tip clearance to be readily accommodated within the design. The effect of tip clearance thus becomes of practical interest.

The introduction of tip clearance above an array results in greater flow area within the channel and thus enables a portion of the coolant to bypass the array rather than proceed through it. All else being equal, this effect will tend to reduce the rate of heat transfer from the array. However, in a liquid cooled scenario, the fins are typically on the order of $H/D \approx 1$, and the surface area of the pin tips can represent a substantial percentage of the overall heat transfer area of the array. Exposing these tips to the fluid tends to promote an increase in overall heat transfer. In addition, some previous work involving tip clearance also suggests that it may promote three-dimensional effects in the flow field, helping to break up the thermal boundary layer along the base of array, thus further increasing heat transfer.

The number of experimental studies considering tip clearance in pin fin arrays is relatively limited. Some of the earliest work relevant to tip clearance in a pin fin array appears to be that of Sparrow et al. [1–3]. They considered [1,2] both inline and staggered arrays with H/D of 1, 2 and 3 with a constant duct height, which resulted in clearance gap to pin length ratios (Cg/H) of 0.14, 0.72 and 2.44. Based on mass transfer from a naphthalene coated pin, they found a decrease in Nu_{pf} of only 20% between the two extreme tip clearances for staggered arrays. The case of no tip clearance was not considered however. They also examined the character of heat transfer at the tip of a single pin fin attached to a wall at only one end [3]. They observed that under this scenario, the rate of heat transfer was higher at and adjacent to the tip of the fin than along the lateral face of the pin away from the tip.

* Corresponding author.
E-mail address: kevin.a.moores@gmail.com (K.A. Moores).

0017-9310/$ - see front matter © 2009 Elsevier Ltd. All rights reserved.
doi:10.1016/j.ijheatmasstransfer.2009.08.005

Nomenclature

A	area (m^2)
Bi	Biot number ($hV_{bp}/k_{bp}A_w$)
C	non-dimensional tip clearance [(Cg/H)100]
Cg	clearance gap (m)
D	average pin diameter (m)
D_H	hydraulic diameter of open channel ($4A/P$) (m)
f	friction factor (Eq. (1))
h	heat transfer coefficient ([W/m^2 K)
H	pin height (m)
k	thermal conductivity (W/mK)
L	length (m)
$\dot{m}$	mass flow rate (kg/s)
N	number of pin rows number of observations (Eq. (6))
Nu	Nusselt number
P	perimeter (m) order of polynomial fit (Eq. (6))
q''	heat flux (W/m^2)
Q	heat rate (W)
Re	Reynolds number
S	pin spacing (m)
SEE	standard estimate of error (Eq. (6))
t	thickness (m)
T	temperature (°C)
U	bulk mean channel inlet velocity (m/s)
V	volume (m^3)
V_{max}	maximum array velocity (m/s)
W	width (m)
Y	experimental value
Y'	predicted value from polynomial

Greek symbols

α	empirical coefficient or exponent
ΔP	pressure drop (Pa)
κ	empirical coefficient or exponent
ν	kinematic viscosity (m^2/s)
ρ	density (kg/m^3)

Subscripts

100	based on 100% fin efficiency
A	array
bp	base plate
$C(0)$	relative to zero tip clearance
$C>0$	relative to positive tip clearance
D	diametral
ew	endwall
f	fluid
h	heater
L	longitudinal direction
p	projected
pf	pin fin
pt	pin tip
T	transverse direction
w	wetted

Jubran et al. [4] considered inline and staggered arrays with (Cg/H) of 0, 0.5 and 1.0, and proposed correlations for each clearance. The reduction in heat transfer between the two extremes was found to be 40%, or twice that reported by Sparrow and Ramsey [1]. Chyu et al. [5] evaluated an array of square pin fins with Cg/H from 0.0 to 2.0 using a transient liquid crystal technique. They found Nu to be only 1.5% lower at $Cg/H = 0.25$ compared to the case with no gap. They also reported increased heat transfer along the endwall, upstream of the array's leading edge, when tip clearance was present. The authors credited the production of vortices along the tips of the pin fins and their subsequent interaction with the endwall for this behavior.

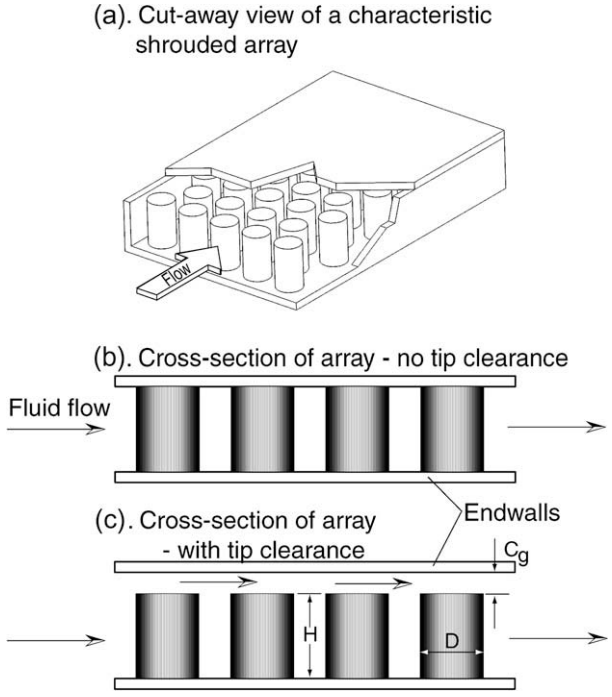

Fig. 1. Shrouded array geometry (a), shown (b) with tip clearance and (c) without tip clearance.

Similarly, Dogruoz et al. [6] considered a series of twenty square pin array geometries with a wide range of S_L/D and Cg/H. Both experimental and numerical work was performed to characterize the impact of clearance on array pressure drop and thermal resistance. A two-branch bypass approach was employed to model differences in hydraulic behavior within the body of the array and the clearance gap above the pins. Experimental heat transfer results were reported as mean array thermal resistances based on thermocouple thermometry. Compared to the non-clearance case, reductions in the rate of heat transfer were reported to be on the order of 5–10% for $Cg/H = 0.5$, and 20–30% at $Cg/H = 3.0$. Based on their modeling, the authors postulated an S_L/D of 2.0 to be optimum in terms of minimizing thermal resistance for the conditions considered.

In a precursor to the current study, Moores and Joshi [7] employed thermocouple thermometry to evaluate the impact of tip clearance for a set of arrays with H/D from 0.5 to 1.1 and Cg/H 0, 0.06, 0.12, 0.18 and 0.25. The study found tip clearance to increase overall rates of heat transfer under some conditions within this clearance range. It was believed that all or most of the improvement could be attributed to the newly exposed pin tip area, with any flow enhancements (such as reported by Chyu) playing only a minor role if any under the conditions studied.

In a recent work by Chang et al. [8] infrared thermometry was employed to measure Nu along the endwall of an array of circular pin fins constructed of a relatively non-conductive material so that heat transfer was primarily from the endwall only. Like Sparrow, they employed a duct of constant height with pins of varying length resulting in H/D from 1.75 to 2.5 and Cg/H of 0, 0.11, 0.25 and 0.43. Empirical correlations for f and Nu were developed. For Cg/H of 0.11, the investigators found Nu_{ew} to be an average of 7%

below that of the non-clearance case, while somewhat surprisingly, f was reported to be reduced to 41% of the non-clearance case.

A summary of these studies is provided in Table 1. Given that the form of Reynolds number used across these works varies somewhat, to provide a point of reference, the authors have included an estimate of the corresponding open channel Reynolds number (Re^*) based on the reported mean flow velocity ahead of the array (U), the hydraulic diameter (D_H) of the open channel, and assuming a representative fluid viscosity (ν) of 1.6×10^{-5} for air and 9.9×10^{-7} for water as appropriate.

In addition to these experimental works, there have been a number of solely numerical studies on the subject of fin tip clearance effects. Among them, Min et al. [9] looked at longitudinal plate fins in a microchannel heat sink geometry scenario. Under the constant pumping power conditions considered in their work, they estimated a 3.5% enhancement in the rate of heat transfer to be achievable at a clearance gap to fin width ratio of 0.6.

More recently, Rozati et al. [10] conducted a systematic numerical study of low Re flow (5–400) and heat transfer in shrouded cylindrical pin fin arrays with and without tip clearance. This study was aimed at micro pin fin cooling schemes which generally require low Re operation to maintain practical levels of pressure loss and pumping power. Their simulations suggested tip clearance effects to be a relatively complex phenomenon. Among their findings, the modeling predicted clearance to be of greatest impact on heat transfer at low Re, and they saw an increase in heat transfer relative to the non-clearance case over some Re and Cg ranges, with decreases in heat transfer under other conditions.

Thus, the primary focus of the current study is to build upon these previous works in understanding the effect of tip clearance, particularly for Cg/H in the range 0–0.25 where heat transfer augmentation has been shown to be achievable. Liquid crystal thermography has been employed on a series of pin fin arrays to evaluate performance based on a full-field temperature analysis as a function of clearance and flow conditions.

2. Experimental apparatus and procedure

2.1. Apparatus

A set of three AlSiC power electronics base plates with H/D of 0.5–1.1 were employed in this study to evaluate the effect of tip clearance on pin fin array heat transfer and fluid flow. Fig. 2 illustrates the plate for the case of $H/D = 1.1$. The plates are commercially manufactured via a molding process that produces a single, homogeneous structure consisting of a 5 mm thick base that is flat on one side and populated with a dense array of 158 pin fins on the other. To facilitate removal from the mold, the pins possess a 4.8° taper angle from base to tip. Consequently, the diameter varies slightly along the length of the pins. The three base plates in this study were geometrically identical apart from pin height. A summary of dimensions is shown in Table 2.

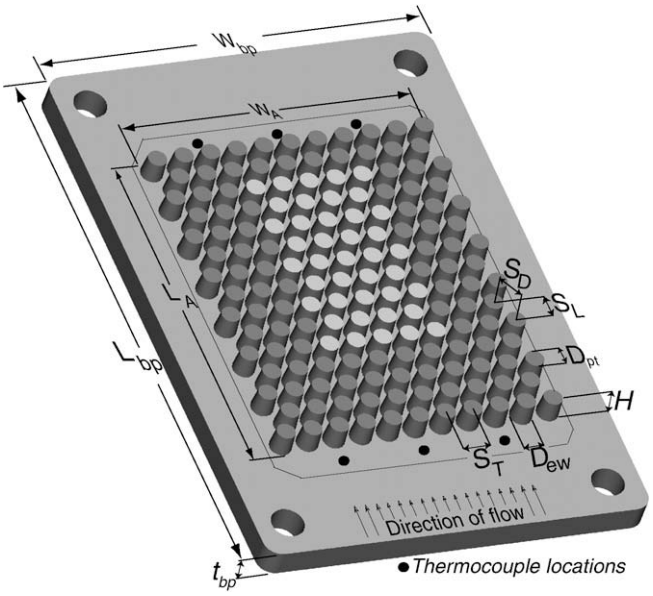

Fig. 2. Base plate geometry.

The thermal and pressure loss performance of each array was evaluated by mounting the base plates on an open channel housing (Fig. 3). The construction of the assembly permits tip clearance to be adjusted from a nominal value of zero to 25% of pin height. The assembly was situated in a closed-loop test facility (Fig. 4). A chiller with integral pump provided distilled cooling water to the test assembly at a constant inlet temperature of 27 °C (±1 °C). A pair of bypass valves was used to control flow rate to the pin fin array. The cooling water passed through a 1 μm filter and then through one of three variable area flow meters operating in parallel prior to entering the assembly, and flowed directly back to the chiller upon exiting the array.

A Sony MD-95 digital camera was mounted perpendicular to the pin fin array, viewing through the clear Plexiglas housing to capture and record the color response of the liquid crystal coated array. A Moritex fiber optic light source and ring light guide (models MFL-150L and MRG61-1500S, respectively) mounted along the same axis of sight as the camera, were used to illuminate the array from directly above. The light source included an infrared filter to limit the amount of heat radiated to the base plate. A tent with black felt walls, represented by the dashed line in Fig. 4, enclosed

Table 1
Summary of experimental conditions considered in the referenced literature.

Reference	H/D	Cg/H	S_T/D	S_L/D	Pin shape	Array orientation	Re definition	Re range	$Re^* = \frac{UD_H}{\nu}$
1	1–3	0.14, 0.72, 2.77	3	2.6	C	S	$\frac{V_{max}D}{\nu}$	1000–9000	5000–35,000
2	1–3	0.14, 0.72, 2.77	3	2.6	C	I	$\frac{V_{max}D}{\nu}$	1000–9000	5000–35,000
3	7–19	0.71	–	–	C	–	$\frac{UD}{\nu}$	2500–25,000	85,000–400,000
4	9.44	0, 0.5, 1.0	2.4–19.5	1.3–11.3	C	S, I	$\frac{G_{max}D}{\nu}$	5000–54,000	12,000–56,000
5	1	0, 0.25, 0.5, 1, 2	2.5	2.5	N	I	$\frac{UH}{\nu}$	16,000	28,000–69,000
6	~1.9	0, 0.25, 0.5, 1, 2, 3	1.75 – 4.1	2.2 – 5.2	N	I	$\frac{U_{mod}L}{\nu}$	210–520	2100–9200
7	0.5–1.1	0, 0.06, 0.12, 0.18, 0.25	~1.33	~1.15	C	S	$\frac{V_{max}D}{\nu}$	200–10,000	100 –4000
8	1.75–2.5	0, 0.1, 0.25, 0.43	2	2	C	S	$\frac{UD_H}{\nu}$	10,000–30,000	10,000–30,000

Variables specific to Table 1: C, cylindrical; N, square; S, staggered; I, inline; G_{max}, max. array mass flow rate; U_{mod}, modified channel velocity; L, unspecified characteristic length.

Table 2
Array geometries and parameters.

Plate	#1	#2	#3
W_{bp} (m), W_A (m)	0.072, 0.054		
L_{bp} (m), L_A (m)	0.106, 0.065		
t_{bp} (mm)	5.0		
H (mm)	2.0	3.0	4.0
D_{ew} (mm)	4.0	4.0	4.0
D_{pt} (mm)	3.67	3.5	3.33
D (mm)	3.84	3.75	3.67
S_T (mm)	5.0	5.0	5.0
S_L (mm)	4.33	4.33	4.33
H/D	0.52	0.8	1.09
S_T/D	1.3	1.33	1.36
S_L/D	1.13	1.15	1.18
A_p (mm^2)	3570	3570	3570
$A_{w,c(0)}$ (mm^2)	3497	4389	5238
$A_{w,c>0}$ (mm^2)	5168	5909	6614
Rows (N)	15		
Pins/row	10 or 11		
k_{bp} (W/m K)	160		

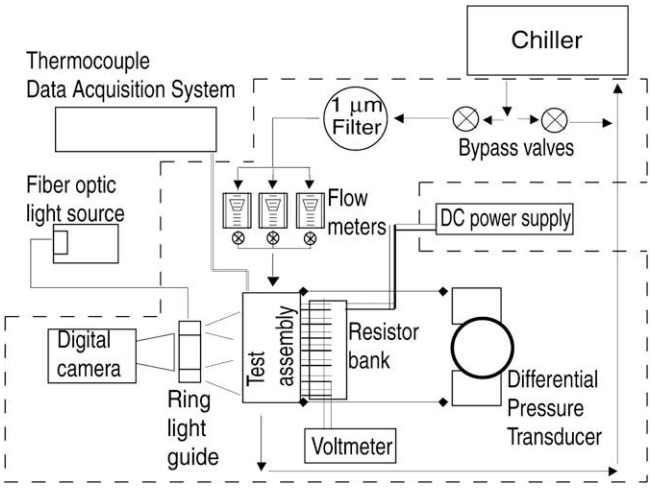

Fig. 4. Schematic of closed-loop test facility.

the major components of the test facility, ensuring that the array was illuminated only by the ring light in a consistent manner throughout testing.

2.2. Test procedures

Thermochromic liquid crystals (TLCs) are materials that exhibit a color change in response to a change in temperature. By applying the material to a given surface and calibrating the temperature-to-color relationship of the liquid crystals, a full-field temperature map of the given object can be produced. A relatively water resistant formulation of microencapsulated liquid crystals manufactured by Hallcrest Inc. was employed in this study. It included C20-10 liquid crystals, AQB-3 binder, and BB-M1 black backing paint. The base plate was coated using an artist's airbrush (Aztek Inc., model A320) with a 0.40 mm nozzle installed. The process of liquid crystal preparation and application employed in this study was based on that described by Farina et al. [11]. Heat transfer tests were conducted over the range of conditions summarized in Table 3. For each individual test, the assembly was manually adjusted to achieve the desired level of nominal tip clearance as described in Moores and Joshi [12]. Each clearance case was tested at 10 flow rates and for each flow, an appropriate level of heat flux was applied to raise the temperature of the array to a point within the color response range of the liquid crystals. Upon reaching steady state for a given flow condition, a series of three digital images were taken at 30 s intervals. Simultaneously, thermocouple readings were taken of the cooling water inlet and outlet temperature, ambient air temperature, and heater block temperature. The thermocouple locations are shown in Figs. 2 and 3.

Table 3
Nominal test conditions.

H/D	0.5, 0.8,1.1
Cg/H	0, 0.06, 0.12, 0.18, 0.25
Re	$2 \times 10^2 - 1 \times 10^4$ (heat transfer) $2 \times 10^2 - 2 \times 10^4$ (pressure loss)
Q_h	59–888 W
q''_{A_p}	1.6–24.4 W/cm^2

2.3. Calibration

The liquid crystals used have a rated response range of 29–33 °C. However during testing, the material was observed to have an actual range of approximately 30.5–35.5 °C. The temperature vs. observed color response of the liquid crystals can be highly dependent on a host of variables including intensity of light, angle of illumination, viewing angle, and even the age of the liquid crystal coating. As a result, in situ calibration is highly recommended (Baughn et al. [13]) to insure accuracy of temperature measurements. For all cases reported here, calibration was performed immediately prior to and immediately following a given experimental trial.

A successive isotherm method based on the hue response of the liquid crystals was employed in this study. With the pin fin array exposed to quiescent cooling water at room temperature, the heater block was powered on. The base plate temperature was allowed to slowly rise to approximately 38 °C, taking care not to heat the crystals more than a few degrees above the maximum demonstrated response temperature to avoid possible hysteresis effects [13]. The heater block was then powered off and the array was allowed to slowly cool down through the temperature activation

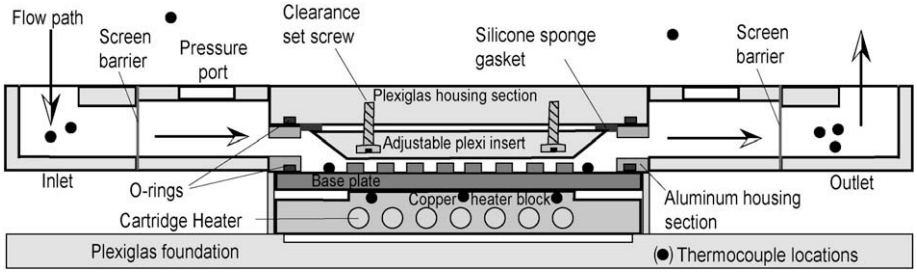

Fig. 3. Cross-sectional view of test assembly.

range of the liquid crystals. This cooling process took approximately 30–45 min due to the considerable thermal mass of the heater and base plate. Under these conditions, the Biot number (Bi) was on the order of 0.01 or less, so the array can be taken as highly isothermal at any given instant throughout the calibration process. During this time, a series of digital images were taken of the array at roughly 0.3 °C increments of temperature drop. Six thermocouples, attached to the endwall of the base plate (Fig. 2), provided a measurement of mean array temperature at the time of each photo.

The digital photos produced by the MD-95 are JPEG images based on an RGB (Red, Green and Blue) color space. These were post-processed using function RGB2HSV of the Matlab image processing library to generate an image based on the HSI (Hue, Saturation and Intensity [Value]) color space. The hue component of the liquid crystal color response was then correlated to temperature separately for each individual pin and its associate endwall area (herein referred to as a unit cell) in order to eliminate any effect of viewing angle. Each array image was subdivided into 158 unit cells with only the central 41 cells (as depicted in Fig. 2) included in the analysis. In doing so, only the fully developed section of the array is included in this study's results.

A typical set of calibration curves is shown in Fig. 5. The results include both the pre-trial and post-trial data together. The degree of difference in the hue-to-temperature relationship between the pin tip and endwall calibration curves in the upper left frame was observed to be directly related to pin height (H) with the difference being almost negligible for $H/D = 0.5$, and increasing as the pin height increased. This is attributed to a shadowing effect during the TLC coating process. For the shorter pins, the coating process produced a uniform and complete TLC coating along both the pin tips and the endwall. With taller pins, shadowing caused a lesser rate of deposition of TLC along the endwall, resulting in less than complete coverage. This in turn caused a downward bias in the hue-to-temperature relationship at the endwall.

At the upper right of Fig. 5, a least square polynomial curve fit was applied to each set of data and used to model the Hue-temperature relationship during the heat transfer trials. The data sets at center left and bottom left show the level of uncertainty associated with the data. The uncertainty in pixel based hue values was also seen to be a direct function of pin height. This too is attributed to the shadowing effect which left some pixel regions with partial or no TLC coverage. While there is significant spread between the hue values of individual pixels, the unit cell average hue value can be seen to change in a consistent and monotonic manner in relation to temperature. For this reason, endwall based heat transfer results have been limited in spatial resolution to the unit cell or larger, which significantly reduces the uncertainty associated with the TLC based results. More localized heat transfer results based on the pin tip regions only are also presented.

In addition to the TLC calibration, a series of tests were performed to quantify non-ideal heat and pressure losses associated with the test assembly [12]. Conduction losses to the foundation and convection losses from wetted areas outside of the array were found to be a maximum of 2% and 15% of total heater block power, respectively, with the highest losses occurring at the low end of the

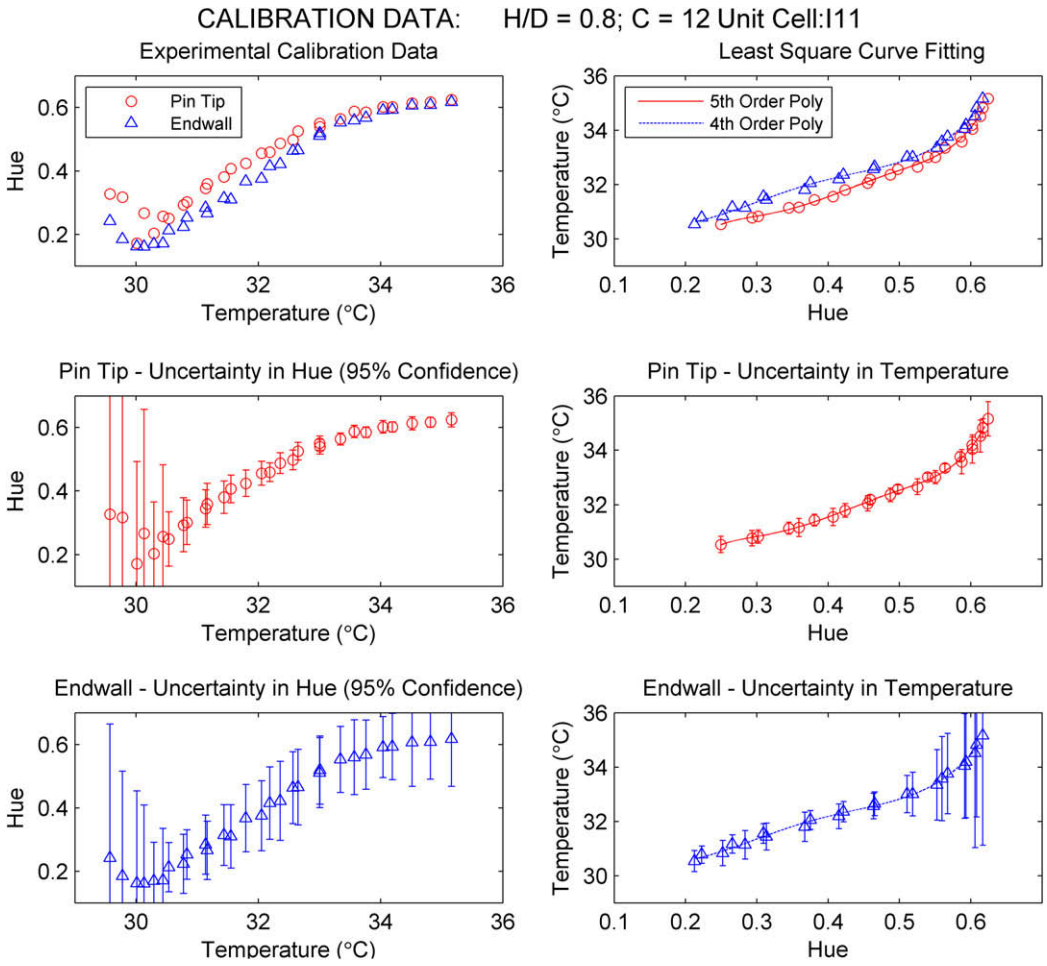

Fig. 5. Typical calibration curves.

Re range. These losses have been correlated to operating conditions and are accounted for in the presented results.

3. Data reduction and uncertainty

3.1. Data reduction

Dimensionless pressure drop results are reported in terms of the friction factor:

$$f = \frac{\Delta P_A}{2\rho_f V_{\max}^2 N} \tag{1}$$

where N is the number of rows in the array.

Heat transfer results are presented primarily in dimensionless form as the Nusselt number (Nu):

$$Nu = \frac{hD}{k_f} \tag{2}$$

where the characteristic length scale of the array is taken to be the average pin diameter (D), as is typical in the pin fin literature, and the heat transfer coefficient (h) is defined as:

$$h = \frac{Q_A}{A(T_{ew} - T_f)} \tag{3}$$

Possible choices of heat transfer area include the total wetted surface area of the pin array (A_w) which would involve all surface area within the borders of the array that is in contact with the cooling fluid, or the projected area of the array (A_p) which is defined as the product of the transverse width and the stream-wise length of the array. Theoretically, A_w experiences a step change between the non-clearance case and those with clearance due to the sudden inclusion of the fin tip area. A_p on the other hand remains constant. Both can be legitimate choices and provide their own unique perspective on performance trends. However, for the given work, A_p has been adopted in all heat transfer calculations.

Both heat transfer and pressure drop results are presented as a function of Reynolds number (Re). Many forms of Re have been used in past studies of shrouded pin fin arrays as indicated in Table 1. In the current study, the form of Re is based on that originally recommended by Zukauskas [14] for analysis of flow across tube banks:

$$Re = \frac{V_{\max} D}{\nu_f} \tag{4}$$

where $V_{\max}$ is the maximum estimated bulk velocity based on the minimum cross-sectional flow area within the array, and is the greater of:

$$V_{\max} = U\frac{S_T(H + Cg)}{(S_T(H + Cg) - HD)} \tag{5a}$$

or

$$V_{\max} = U\frac{S_T(H + Cg)}{2(S_D(H + Cg) - HD)} \tag{5b}$$

Eqs. (5a) and (5b) have been modified from that of Zukauskas to account for the presence of tip clearance. For the geometries considered in this study, scenario (5a) produced the minimum flow area for all cases and is illustrated in Fig. 6. It should be noted that in adopting this definition, any significant differences in local mean velocity between the body of the array and that above the array when tip clearance is present is not accounted for. Instead, the concept of a mean bulk velocity across the entire cross-sectional flow area as is typically used for non-clearance situations is also extended to the clearance scenario. While perhaps not ideal, this approach is consistent with that employed by previous authors [1,2].

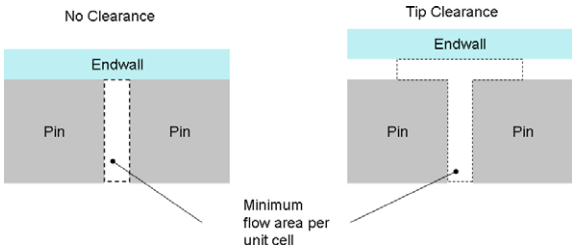

Fig. 6. Unit cell based minimum flow areas.

3.2. Estimated uncertainties

A summary of uncertainties determined to a confidence level of 95% is given in Table 4. Thermocouple based uncertainty measurements were determined through direct calibration using an ice bath and a precision thermometer with 1/20 °C gradation. Liquid crystal based temperature uncertainties associated with each unit cell are taken to be a root mean square (RMS) combination of the thermocouple uncertainties and the standard estimate of error (SEE) associated with each polynomial curve fit to the liquid crystal calibration data determined as:

$$SEE = \sqrt{\frac{\sum(Y - Y')^2}{N - P}} \tag{6}$$

All other reported uncertainties have been determined using the approach of Kline and McClintock [15] assuming uncertainties associated with array and channel dimensions to be negligible. The highest uncertainties in heat transfer occurred at the low end of the Re range (<1000). Through the majority of the flow range, uncertainties in Nu were typically on the order of 6–8%.

4. Results and discussion

4.1. Pressure loss

In an attempt to correlate the pressure data to changes in clearance, a power law relationship was assumed as is commonly employed in the literature for pin fin arrays [16,17]. In the current study, this relationship takes the form:

$$f = \alpha_0\left(\frac{H}{D}\right)^{\alpha_1}\left(1 + \frac{Cg}{D}\right)^{\alpha_2} Re^{\alpha_3} \tag{7}$$

A non-linear multiple regression analysis was performed to determine the most appropriate coefficients and exponents for the given data. The result is shown in Fig. 7. It can be seen that the correlation does a fairly good job of predicting the non-clearance data, but performs more poorly relative to the clearance cases.

Table 4
Estimated uncertainties.

Variable	Maximum uncertainty
T (thermocouples)	±0.13 °C
T (liquid crystals)	±0.39 °C
ΔP	±1.1%
$\dot{m}$	±2.4%
Q_H	±0.4%
Re	±3.6%
Nu	±13.0%
f	±4.5%

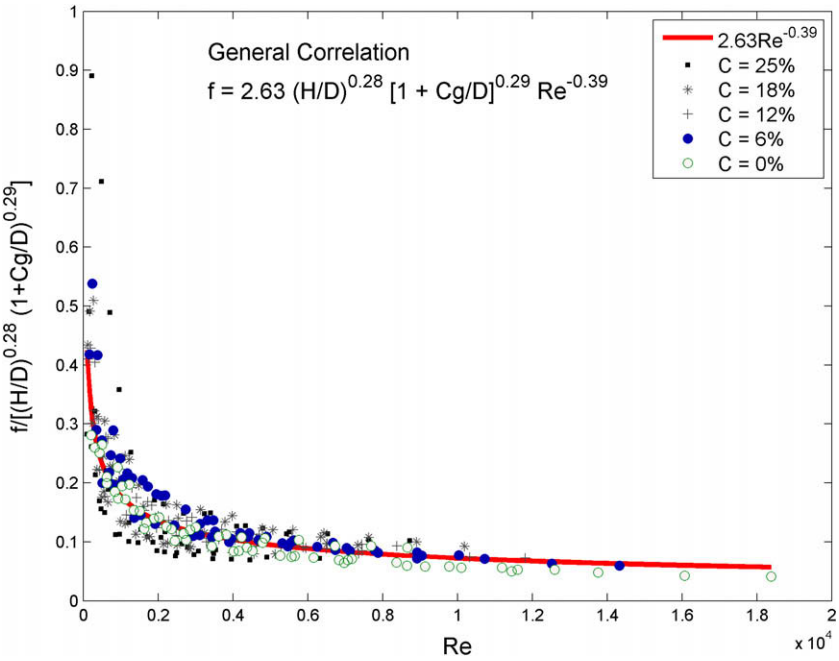

Fig. 7. General power law correlation of non-dimensional pressure loss data.

More specifically, the clearance data for $Cg/H = 0.06$ and 0.12 tend to be under-predicted by the correlation while that for $Cg/H = 0.18$ and 0.25 are over-predicted.

The results indicate that on a *Re* basis there is an initial increase in pressure drop with the introduction of low levels of clearance on the order of 10% of pin height or less. At higher levels of clearance, the pressure loss drops below that experienced when no clearance is present. This general behavior is consistent with the numerical study of Rozati et al. [10]. They credited the initial increase in pressure drop to "...a larger increase in wall shear stresses than the corresponding decrease in form losses", referring to the impact of shroud area above the tip that becomes exposed to the fluid with the introduction of tip clearance. The data of Fig. 7 also suggests that the impact of clearance is greatest at low *Re*, with the greatest impact occurring below $Re = 5 \times 10^3$.

While the standard power law correlation does not effectively capture the impact of clearance, the data is not entirely random either. There does appear to be a general pattern to the data. Upon correlating each individual set of clearance data to Eq. (7), (less the clearance parameter), it was observed that the coefficients and exponents closely followed a direct exponential relationship with the degree of clearance present. This leads to the proposal of a modified power law correlation such that:

$$f = 2.63\kappa_1 \cdot \left(\frac{H}{D}\right)^{0.28+(1-\kappa_1)} Re^{-0.39+(1-\kappa_2)} \tag{8}$$

where:

$$\kappa_1 = e^{4.3(Cg/H)} \tag{8a}$$

$$\kappa_2 = e^{0.8(Cg/H)} \tag{8b}$$

$$Cg/H \leq 0.26 \tag{8c}$$

In this form, the correlation, as shown in Fig. 8, is able to predict both clearance and non-clearance data to within ±21% at a confidence level of 95% for all $Cg/H \leqslant 0.19$ and ±32% for larger clearances considered here. This represents a roughly twofold reduction in uncertainty compared to the standard power law correlation in Fig. 7.

4.2. Mean heat transfer

The observed heat transfer is presented in Fig. 9. Given that *Nu* is based on the projected area of the array, the results correspond to heat transfer rates as would be experienced by an electronic component mounted on top of the baseplate, and are not local rates along the wetted surface of the array. Power law based trend lines of the form

$$Nu = \alpha_0 Re^{\alpha_1} \tag{9}$$

are fit to each individual data set. Results for $H/D = 0.5$ and Cg/H of 0% and 6% are not presented since the array temperatures under test fell outside the calibrated range of the TLC and therefore did not produce valid results.

In the case of $H/D = 0.8$ an improvement in mean heat transfer was achieved for a majority of the clearance cases when compared to the equivalent non-clearance scenario. However, for the case of $H/D = 1.1$, the opposite was the case with the vast majority of clearance trials underperforming compared to the non-clearance operation. This apparent inconsistency arises due to the differences in pin fin efficiency between the two cases. The lower efficiency of the longer pins limits the effectiveness of the exposed pin tip areas, resulting in an overall reduction in mean heat transfer.

Employing TLC temperature readings from the endwall and pin tip areas, an effective fin efficiency can be estimated. Given that the fins in this study do not adhere to all of the so called Murray–Gardner [18,19] assumptions for fin analysis, the authors chose to apply a simple linear temperature profile along the length of the pins. Applying these results to the observed data, efficiency corrected behavior is determined (corresponding to 100% fin efficiency) as illustrated in Fig. 10. Once differences in conduction effects are accounted for, the mean heat transfer rate is seen to increase in the majority of clearance cases for both pin aspect ratios ($H/D = 0.8$ and 1.1). This indicates that for tip clearance to play a constructive role, the array must be of a highly conductive nature, operate at a relatively low rate of convective heat transfer, or both in order to maximize the temperature excess at the tip.

Because forced convection liquid cooling systems require a pump that can represent a significant portion of system cost both

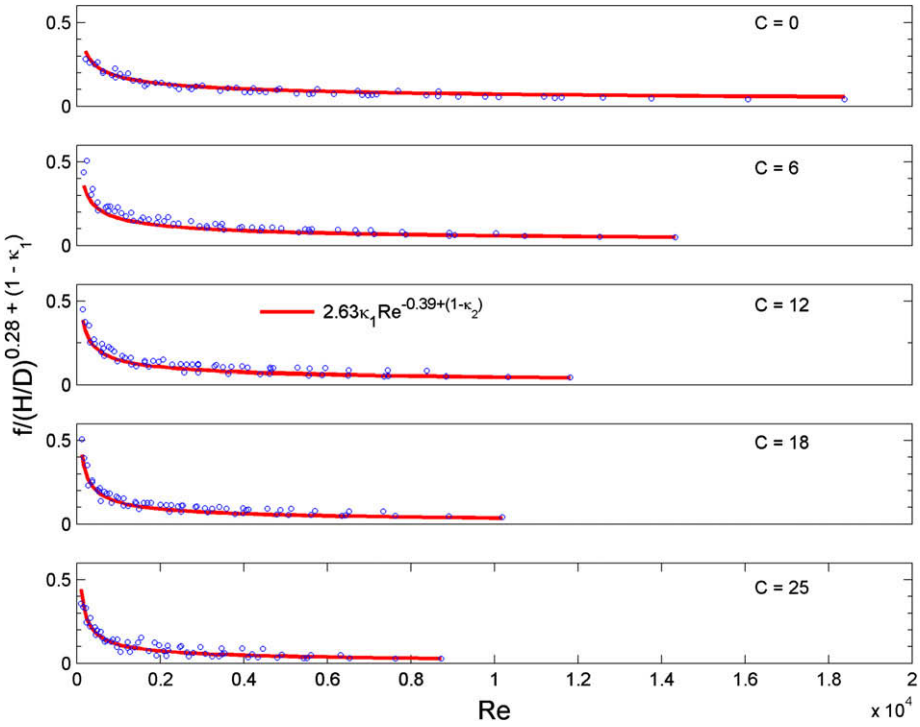

Fig. 8. Modified general correlation of friction factor (f) vs. Re, Cg/H, H/D.

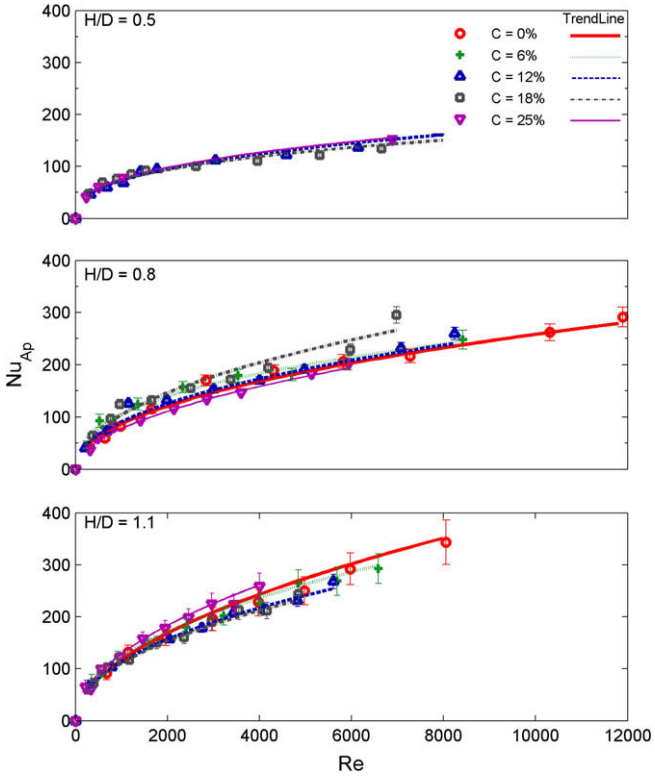

Fig. 9. Nu_{A_p} vs. Re for all H/D and C.

in terms of initial investment, operating costs, and even maintenance costs, a practical engineering consideration would be the behavior of heat transfer relative to tip clearance for a given pumping power. Fig. 11 illustrates the expected relative change in heat transfer for each clearance setting when compared to the case with no clearance assuming the same pumping power in both cases. The power law correlations fit to each individual data set of f and Nu were employed to estimate heat transfer rate and pumping power for a given combination of Re and H/D and zero tip clearance. With pumping power then fixed at the given value, the correlations were used to estimate the Re associated with that power level and the resulting heat transfer at each clearance setting. The results were plotted on the basis of $Re_{C(0)}$ which is the Reynolds number associated with zero tip clearance. Given that no heat transfer results were available for $Cg/H = 0\%$ and 6% for $H/D = 0.5$, results are only presented for the arrays of $H/D = 0.8$ and 1.1.

Fig. 11 paints a complex picture, but several relationships are evident. In the case of $H/D = 0.8$, the minimum clearance gap results in an improvement in relative heat transfer up to 35% in the laminar region, but it gradually decreases until it dips below unity around $Re = 6000$. Successive increases of Cg/D to 10% and 14% exhibit both a reduction in the rate of change in relative heat transfer across the given Re range, combined with a trend towards increased relative heat transfer for all Re. This is likely an indication that the tip area becomes fully engaged in heat transfer between these two clearance gaps. At the maximum clearance of $Cg/D = 0.2$, a significant reduction is observed at all Re, with relative heat transfer slightly below unity. In the case of $H/D = 1.1$, similar trends are apparent with the exception of $Cg/D = 0.27$, which was observed to produce ~40% increase in relative heat transfer through the majority of the range.

This trend towards increased heat transfer per unit pumping power was also reflected in the numerical results of Rozati et al. [10]. The relative degree of augmentation determined in that study was somewhat higher, though the Re range considered was quite low, which may explain the discrepancy given that the impact of tip clearance appears to be greatest at low Re.

4.3. Local heat transfer

The full field nature of the liquid crystal results can be useful in inferring changes in flow field due to the introduction of tip

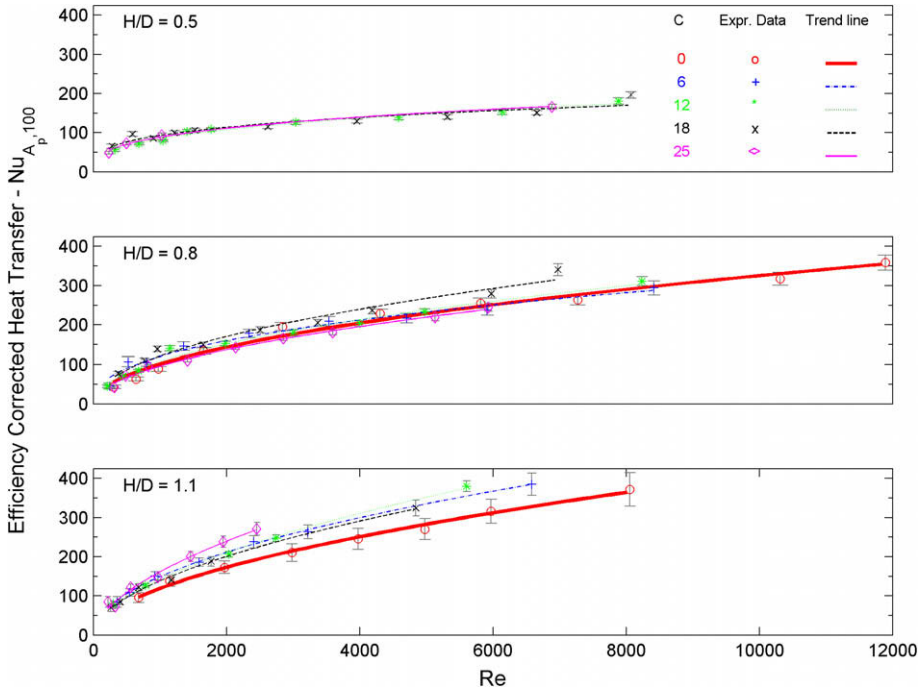

Fig. 10. Efficiency corrected heat transfer results, A_p basis.

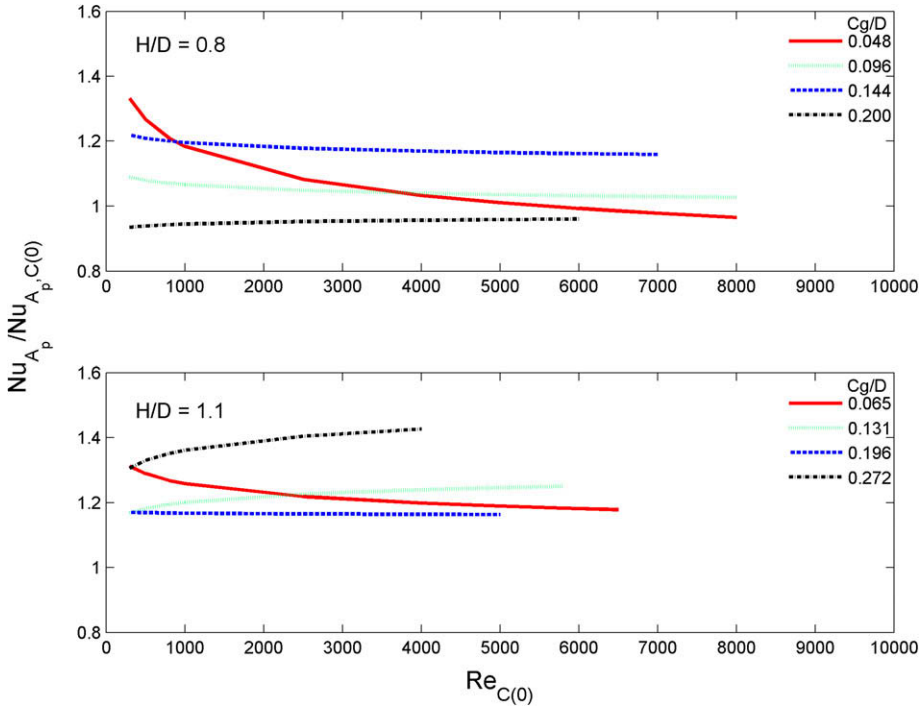

Fig. 11. Impact of clearance given a constant pumping power.

clearance. Fig. 12 shows the temperature profile of an array with and without tip clearance at relatively equivalent flow and heat transfer conditions which are summarized in Table 5. The gray-scale images are comprised of individual pixel hue values normalized to a 0–1 scale. The darker regions represent lower hue values and thus lower temperatures, while lighter regions correspond to higher hue values and temperatures. In each case, the direction of flow is from bottom to top.

A distinct difference in pin tip temperature profile was observed between the case of no clearance and those with clearance. In the case of $Cg/H = 0$, the temperature field across the pin tips varied mostly in the flow direction. The temperature distribution for $Cg/H = 0.18$ on the other hand, exhibited a maximum temperature region along the center of the pin in the flow direction. Also, while the temperature field for the non-clearance case was relatively invariant, when clearance was present it was observed to be

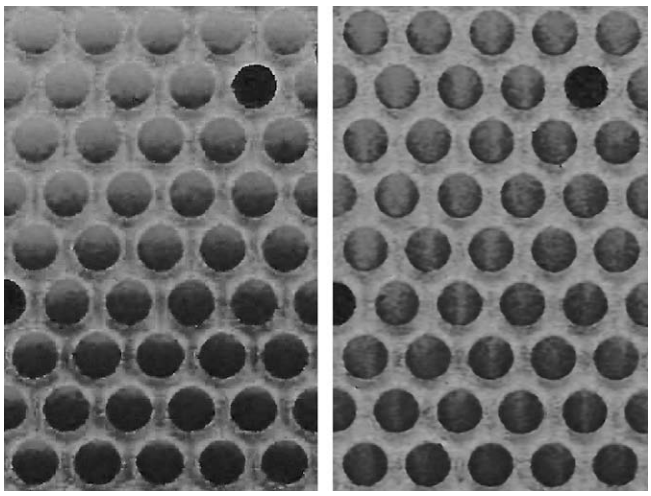

Fig. 12. Grayscale liquid crystal images based on pixel hue values. Left image ($Cg/H = 0.0$), Right image ($Cg/H = 0.18$).

Table 5
Conditions depicted in Fig. 12.

	Left image	Right image
H/D	0.8	0.8
Cg/H	0.0	0.18
Re	1382	1384
q''_{A_p} (W/cm^2)	6.50	7.36

periodic in nature, with regions of elevated temperature appearing to "wash over" the central portion of the pin tips at a frequency of several seconds.

Detailed temperature maps for the center pin of each image are shown in Figs. 13 and 14. Each pin tip exhibits a temperature range from approximately 31.7–33.2 °C. With no clearance, the temperature at the tip rises uniformly and in a near linear fashion along the direction of flow, reaching a maximum near the trailing edge. With $Cg/H = 0.18$, the temperature field is in the form of a hillock, with the crest running through the center of the tip in the stream-wise direction. Rozati et al. [10] observed similar thermal behavior as shown in Fig. 15. The profile on the left illustrates the expected pin tip temperature field at $Re = 10$. While the scenario includes tip clearance, given the extremely low local velocities along the pin tip face at this condition, one would expect this situation to approximate the non-clearance case where there is no flow across the face. Fig. 15(b), on the other hand, shows the temperature distribution with significantly higher bulk velocities ($Re = 325$). In both cases, the model is in close qualitative agreement with the current experimental results. Rozati credited flow acceleration through the gap along with pin tip-wake interactions for this behavior.

5. Summary and conclusions

The primary aim of this study was to provide a systematic experimental evaluation of pin fin array performance with small pin tip clearance gaps of 0–25% of pin height. The results obtained have been presented and discussed in terms of the impact to both pressure drop and heat transfer of the array and can be summarized as follows:

5.1. Pressure loss behavior

- On a non-dimensional basis, the overall pressure drop was found to initially increase with the introduction of tip clearances for $0.05 < Cg/D < 0.10$. For $Cg/D > 0.10$ the pressure drop was generally lower than that of the non-clearance case, in line with recent numerical results produced by Rozati et al. [10]. The impact of clearance on the non-dimensional pressure drop (f) was also observed to decrease with increasing Reynolds number. At the low end of the Reynolds number range considered ($Re \sim 200$), f was observed to be as much as 50% greater with clearance than without it, while the presence of tip clearance appeared to have little appreciable impact on friction factor for $Re > 5000$.

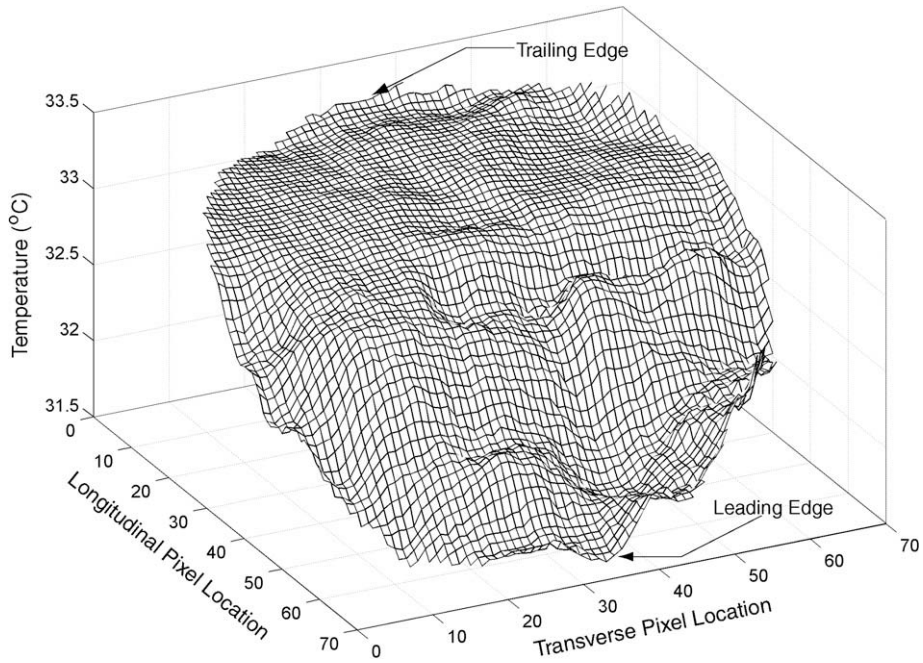

Fig. 13. Pin tip temperature field, $Cg/H = 0$.

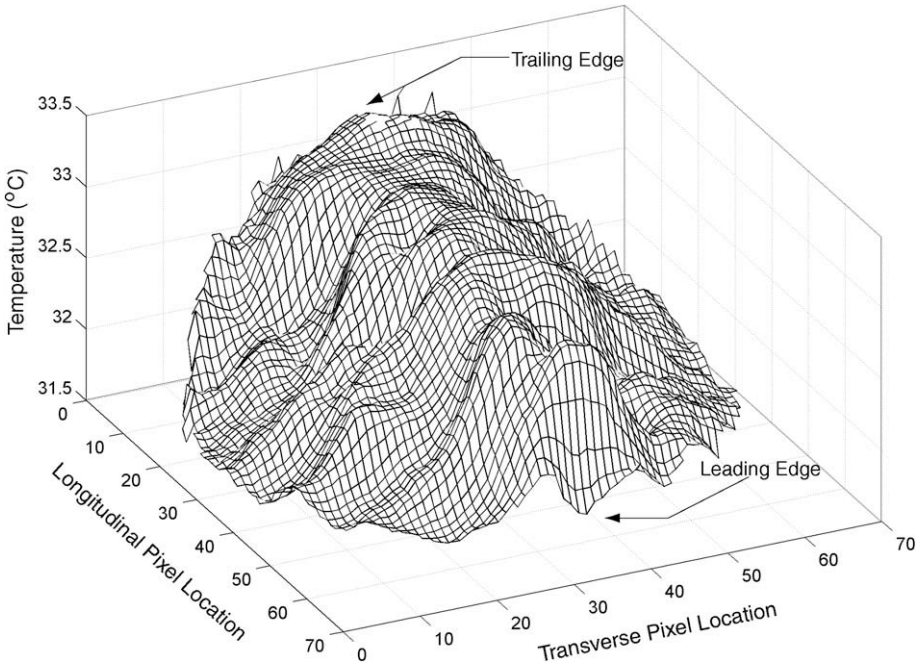

Fig. 14. Pin tip temperature field, $Cg/H = 0.18$.

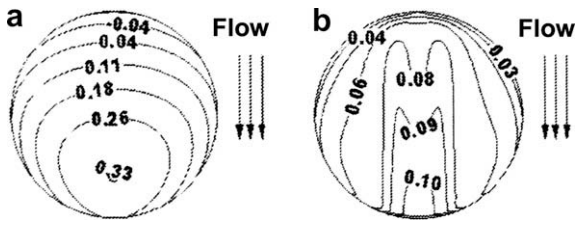

Fig. 15. Numerically predicted non-dimensional pin tip temperature profile for (a) $Re = 10$, $Cg/D = 0.3$ and (b) $Re = 325$, $Cg/D = 0.3$ [10]).

- It was observed that the standard power law relationship which has typically been employed to empirically model flow and heat transfer effects in pin fin arrays is insufficient to model the effects of clearance accurately. An empirical correlation based on a modified power law relationship that employs an exponential function of Cg/H has been proposed. This correlation was shown to produce a $2\times$ improvement in accuracy compared to the standard power law form.

5.2. Heat transfer behavior

- On a constant volumetric flow rate basis, heat transfer rates were observed to be greatest when no tip clearance was present. On a *Re* (i.e. constant local velocity) basis, increases in heat transfer are possible. Whether an increase or decrease occurs, and what the relative degree of the change will be, appears to be a complicated function of *Re*, Cg/D, H/D, assuming other array parameters are invariant. On a constant pumping power basis, the inclusion of tip clearance was found to be generally advantageous within the range of tip clearance considered, particularly in the laminar range. As *Re* increased the relative impact of clearance in most cases was seen to decrease, with some clearance values resulting in a slightly lower heat transfer per pumping power than at the non-clearance case.
- Liquid crystal imaging provided visual evidence of basic changes in fluid flow about the pin tips which supports the numerically based predictions of Rozati et al. [10]. It was observed that with the introduction of clearance, the pin tips experience transient fluctuations in flow patterns with presumed vortices washing across the outer edges of the pin tips, producing an elongated vertical temperature profile along the stream-wise length of the tip. This is in contrast to a horizontal temperature field observed for the non-clearance case.

References

[1] E.M. Sparrow, J.W. Ramsey, Heat transfer and pressure drop for a staggered cylinder wall attached array of cylinders with tip clearance, Int. J. Heat Mass Transfer 21 (1978) 1369–1377.
[2] E.M. Sparrow, J.W. Ramsey, C.A.C. Altemani, Experiments on in-line pin fin arrays and performance comparisons with staggered arrays, J. Heat Transfer 102 (1980) 44–50.
[3] E.M. Sparrow, F. Samie, Measured heat transfer coefficients at and adjacent to the tip of a wall-attached cylinder in cross-flow: application to fins, J. Heat Transfer 103 (1981) 778–784.
[4] B.A. Jubran, M.A. Hamdan, R.M. Abjualh, Enhanced heat transfer, missing pin, and optimization for cylindrical pin fin arrays, J. Heat Transfer 115 (1993) 576–583.
[5] M.K. Chyu, C.H. Yen, W. Ma, T.I.P. Shih, Effects of flow gap atop pin elements on the heat transfer from pin fin arrays, 99-GT-47, ASME Gas Turbine & Aeroengine Expo, 1999, June 7–10, Indianapolis, Indiana.
[6] M.B. Dogruoz, M. Urdaneta, A. Ortega, Experiments and modeling of the hydraulic resistance and heat transfer of in-line square pin fin heat sinks with top by-pass flow, Int. J. Heat Mass Transfer 48 (2005) 5058–5071.
[7] K.A. Moores, Y.K. Joshi, Effect of tip clearance on the thermal and hydrodynamic performance of a shrouded pin fin array, J. Heat Transfer 125 (2003) 999–1007.
[8] S.W. Chang, T.L. Yang, C.C. Huang, K.F. Chiang, Endwall heat transfer and pressure drop in rectangular channels with attached and detached circular pin-fin array, Int. J. Heat Mass Transfer 51 (2008) 5047–5259.
[9] J.Y. Min, S.P. Jang, S.J. Kim, Effect of tip clearance on the cooling performance of a microchannel heat sink, Int. J. Heat Mass Transfer 47 (2004) 1099–1103.
[10] A. Rozati, D.K. Tafti, N.E. Blackwell, Effect of pin tip clearance on flow and heat transfer at low Reynolds numbers, J. Heat Transfer 130 (2008) 071704.
[11] D.J. Farina, J.M. Hacker, R.J. Moffat, J.K. Eaton, Illuminant invariant calibration of thermochromic liquid crystals, HTD-252, Vis. Heat Transfer Process. (1993) 1–11.
[12] K.A. Moores, Effect of tip clearance on the thermal and hydrodynamic performance of shrouded pin fin arrays, Ph.D. thesis, University of Maryland, College Park, MD, 2008.
[13] J.W. Baughn, M.R. Anderson, J.E. Mayhew, J.D. Wolf, Hysteresis of thermochromic liquid crystals temperature measurement based on hue, J. Heat Transfer 121 (1999) 1067–1074.

[14] A.A. Zukauskas, Heat transfer from tubes in cross-flow, Advances in Heat Transfer, vol. 8, Academic Press, New York, 1972.
[15] SJ. Kline, F.A. McClintock, Describing uncertainties in single sample experiments, Mech. Eng. 75 (1953) 3–8.
[16] D.E. Metzger, Z.X. Fan, W.B. Shephard, Pressure loss and heat transfer through multiple rows of short pin fins", ASME Paper No. 82-IHTC-31, 1982, pp. 137–142.
[17] B.E. Short, Pressure drop and heat transfer in cast pin fin coldwalls, Ph.D. Thesis, Southern Methodist University, Dallas, TX, 1994.
[18] W.M. Murray, Heat dissipation through an annular disk of fin of uniform thickness, J. Appl. Mech. 5 (1938) A78–A80.
[19] K.A. Gardner, Efficiency of extended surfaces, Trans. ASME 67 (1945) 621–631.